Journal of Power Sources 185 (2008) 423–427

Contents lists available at ScienceDirect

Journal of Power Sources

journal homepage: www.elsevier.com/locate/jpowsour

Short communication

Graphitic mesoporous carbon as a durable fuel cell catalyst support

Paul V. Shanahan[a], Lianbin Xu[a,b], Chengdu Liang[c], Mahesh Waje[a], Sheng Dai[c,*], Y.S. Yan[a,*]

[a] Department of Chemical and Environmental Engineering, University of California, 900 University Avenue, Riverside, CA 92521, USA
[b] Key Lab for Nanomaterials, Ministry of Education, Beijing University of Chemical Technology, Beijing 100029, China
[c] Chemical Sciences Division, Oak Ridge National Laboratory, Oak Ridge, TN 37831, USA

ARTICLE INFO

Article history:
Received 4 March 2008
Received in revised form 2 June 2008
Accepted 10 June 2008
Available online 22 June 2008

Keywords:
Catalyst support
Durability
Fuel cell
Graphitic carbon
Mesopores
Carbon black

ABSTRACT

Highly stable graphitic mesoporous carbons (GMPCs) are synthesized by heat-treating polymer-templated mesoporous carbon (MPC) at 2600 °C. The electrochemical durability of GMPC as Pt catalyst support (Pt/GMPC) is compared with that of carbon black (Pt/XC-72). Comparisons are made using potentiostatic and cyclic voltammetric techniques on the respective specimens under conditions simulating the cathode environment of PEMFC (proton exchange membrane fuel cell). The results indicate that the Pt/GMPC is much more stable than Pt/XC-72, with 96% lower corrosion current. The Pt/GMPC also exhibits a greatly reduced loss of catalytic surface area: 14% for Pt/GMPC vs. 39% for Pt/XC-72.

1. Introduction

Carbon-supported platinum (Pt) catalysts are the most commonly used electrocatalysts in proton exchange membrane fuel cells (PEMFCs). An issue of paramount importance for fuel cell operation is their performance over extended periods (i.e., durability) [1–9]. Catalytic activity is directly proportional to the available Pt surface area of the catalyst. Loss of carbon support due to corrosion is one of the main causes of loss of active Pt surface area [1,4].

Carbon black as the catalyst support is a mainstay in PEMFCs, but the adverse operating conditions (i.e., low pH, high electrical potential, high humidity and high temperature), as well as the presence of Pt, within the catalyst layer amplify the corrosion of the carbon support [1,5]. The key structural deficiencies associated with carbon black are: broad pore-size distribution with a significant portion being micropores (pore size < 2 nm), low degree of graphitization, and the presence of surface functional groups. Pt nanoparticles deposited in the micropores are inaccessible for electrocatalysis, leading to low Pt utilization. The low degree of graphitization is the key factor affecting the electrical conductivity and stability of membrane electrode assemblies (MEAs). The high content of surface functional groups facilitates the oxidative corrosion of carbon supports. The loss of support releases the Pt nanoparticles; the nanoparticles either aggregate or migrate away from the triple phase boundaries. In either case, it results in loss of active Pt surface area. Carbon nanotubes (CNT) have been considered as a possible replacement for carbon black and have been shown to be more corrosion-resistant than carbon black [6], but the cost of manufacturing carbon nanotubes, whether it be single-walled, double-walled or multi-walled nanotubes, is a significant concern.

A viable alternative to carbon black and CNTs is mesoporous carbons (MPCs) containing monodispersed mesopores (pore size > 2 nm). Recently, Ryoo and co-workers have demonstrated that MPCs prepared by hard-template synthesis are very effective in dispersing Pt nanocatalysts through a space confinement imposed by mesopores [10]. However, the degree of graphitization for these MPCs is very similar to that of carbon black and therefore they suffer similar corrosion problems. The graphitization of the MPCs derived from hard-template synthesis at high temperature (>2000 °C) can lead to the collapse of the corresponding mesostructures because of their intrinsic absence of strong pore-wall structures [11]. The pore-walls of these MCPs are held together through thin carbon filaments.

A new dimension in ordered mesoporous carbons has been opened up with the development of a synthesis method based on a soft-template [12–14]. Unlike the MPCs derived from a hard-template, the MPCs derived from a soft-template entail strong pore-wall structures, utilizing polymer templates and carbon precursors [12]. They are expected to retain their mesostructures

* Corresponding authors. Tel.: +1 951 827 2068; fax: +1 951 827 5696.
E-mail addresses: dais@ornl.gov (S. Dai), Yushan.Yan@ucr.edu (Y.S. Yan).

0378-7753/$ – see front matter © 2008 Elsevier B.V. All rights reserved.
doi:10.1016/j.jpowsour.2008.06.041

and associated surface area under harsh graphitization conditions, leading to graphitic mesoporous carbons (GMPCs) with considerably enhanced chemical stability [14]. Since the GMPCs are a graphitic form of carbon, they share many of the attractive features of CNTs. For example, they have high surface area of ~300 $m^2\,g^{-1}$ and low electrical resistivity of 3 mΩ cm after heat-treatment at 2400 °C. Their resistivity is much higher after a low temperature heat-treatment, e.g., 4 Ω cm after heat-treatment at 850 °C. GMPCs are significantly less costly to produce than CNTs. In this work, we report the fabrication of GMPC by simply heat-treating polymer-templated MPC at high temperature, and examine the corrosion current of GMPC-supported Pt (Pt/GMPC) under conditions simulating the cathode environment of PEMFC. By comparing the electrochemical properties of Pt/GPMC with Pt/XC-72 (Vulcan XC-72 supported Pt), it is found that the use of GPMC can be promising in effectively reducing the loss of catalytic surface area.

2. Experimental

2.1. Synthesis of GMPCs

The pre-graphitization MPCs were prepared through a soft-template method as reported previously [14]. In brief, 2.52 g phloroglucinol and 2.52 g polyethyleneoxide-*b*-polypropyleneoxide-*b*-polyethyleneoxide (Pluronic F127 EO_{106}–PO_{70}–EO_{106}) were dissolved in 18 g of a mixture of ethanol, water, and 37% HCl with a weight ratio of 10:9:0.1. 2.6 g of 37% formaldehyde solution was then added to the mixture in one batch and stirred for 1 h. A polymer layer was separated from the reactants and cast into a thin film on a 15-cm OD Petri dish. The film was further cured at 80 °C for 12 h after it was dried overnight at room temperature. The cured film was scratched off the Petri dish and carbonized under nitrogen in a tubular furnace, which was ramped to 850 °C at 1 °C min^{-1} and then kept at 850 °C for 2 h. Afterwards, the carbonized sample was heat-treated at 2600 °C for 1 h under helium in a graphite furnace to produce GMPCs. The pores within the GMPCs are tunable on the order of 6–15 nm. The GMPCs studied here, have pores of ~9 nm.

2.2. Characterization of GMPCs

The structures of the carbon materials before and after heat-treatment were characterized by X-ray diffraction (XRD) analysis using a Bruker AXS D8 Advance diffractometer with Cu Kα radiation ($\lambda_{K\alpha 1}$ = 1.5418 Å), and Raman spectroscopy using a Dilor XY laser Raman spectrometer. The specific surface areas of the GMPCs were measured by Brunauer–Emmett–Teller (BET) method of nitrogen sorption at liquid nitrogen temperature (77 K) using a Micromeritics ASAP 2010 Accelerated Surface Area and Porosimetry Analyzer. The pore-size distributions were calculated by Barrett–Joiner–Halenda (BJH) method by using the adsorption branches of the BET curves.

2.3. Deposition of platinum on GMPCs

A very appealing feature of the GMPCs was the ease of which nanometer-sized catalyst particles could be deposited on the support. Platinum particles of about 2–3 nm were produced using a chloroplatinic acid/acetone solution [10]. 200 mg of $H_2PtCl_6{\cdot}6H_2O$ (37.5 wt% Pt) were dissolved in a 4 mL of acetone, 300 mg ground graphitic mesoporous carbon (particle size ~5 μm) were then placed in the solution and ultrasonicated for 1 h in order to drive out any air bubble that might be trapped in the pores. It was then dried overnight under a light vacuum (~37 mmHg gauge pressure). The resulting dry powder was placed in a ceramic boat and reduced at 150 °C for 1 h in hydrogen/argon with a gas flow of 100 ssc min^{-1} of Ar and 30 ssc min^{-1} of H_2.

2.4. Determination of catalyst loading and thermal stability

Catalyst loading of the Pt/GMPC and thermal stability of the two catalysts (Pt/GMPC and 20 wt% Pt/XC-72 (E-TEK)), was determined by thermogravimetric analysis (TGA) of the various samples (i.e., Vulcan XC-72, 20 wt% Pt/XC-72, GMPC, or 18 wt% Pt/GMPC), using a Mettler-Toledo TGA/SDTA 851e thermobalance. Samples of approximately 4–5 mg were heated in air with a flow rate of 50 mL min^{-1} from 25 to 400 °C at 10 °C min^{-1}, followed by a 15-min soak, then from 400 to 800 °C at 10 °C min^{-1}, followed by an 30-min soak.

2.5. Electrochemical measurements

The electrochemical measurements were performed in a three electrode electrochemical cell utilizing a rotating disk working electrode setup with a double junction Ag/AgCl/KCl (satd.) reference electrode and a platinum wire counter electrode. The working electrode was prepared by casting the ink onto a 5-mm diameter glassy carbon disk electrode (Pine Instrument). The ink was produced by ultrasonically dispersing 8.0 mg specimen (i.e., Vulcan XC-72, 20 wt% Pt/XC-72, GMPC, or 18 wt% Pt/GMPC) in 4.0 mL ethanol for 30 min. 50 μL ink was then pipetted onto the disk electrode. After drying the ink at 80 °C, 40 μL of a 0.05 wt% Nafion® solution (diluted from 5 wt%, Ion Power, Inc.) was pipetted on the electrode surface in order to affix the catalyst particles onto the glassy carbon substrate.

The support oxidation experiments were carried out at 25 °C in argon purged 0.5 M H_2SO_4, by applying a constant potential (0.9 V) using a VMP2 potentiostat (Princeton Applied Research); chronoamperometric recordings were taken for 16 h. All potentials herein are reported vs. double junction Ag/AgCl/KCl (satd.) reference electrode at 25 °C. Cyclic voltammetry (CV) was performed on the two supported catalyst specimens (i.e., 20 wt% Pt/XC-72 and 18 wt% Pt/GMPC) in order to determine the active surface area of the Pt. The voltage was swept from −0.21 to 0.8 V, at a sweeping rate of 50 mV s^{-1}. Extended corrosion experiments were performed for 160 h. During these extended corrosion tests, CV was recorded at regular intervals to determine the corrosion effect on the Pt active surface area.

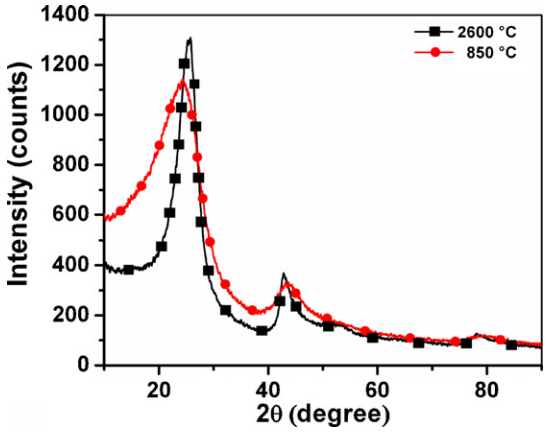

Fig. 1. XRD patterns of the MPC before (●) and after heat-treatment (■) at 2600 °C.

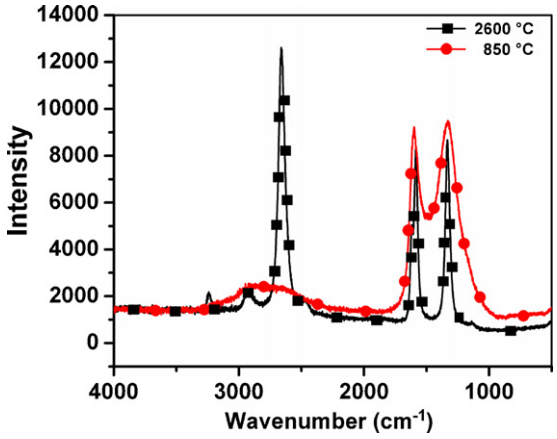

Fig. 2. Raman spectra of the MPC before (●) and after heat-treatment (■) at 2600 °C.

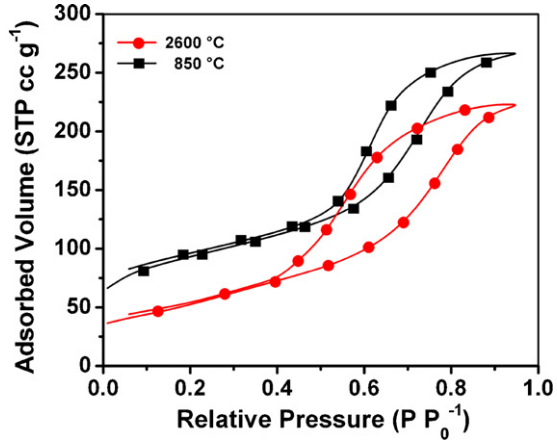

Fig. 3. N_2 adsorption/desorption isotherms of the MPC before (●) and after heat-treatment (■) at 2600 °C.

2.6. Morphology and Pt particle size of Pt/GMPC

The microscopic features of Pt/GMPC were examined by high resolution transmission electron microscopy (HRTEM) using a Philips CM300 microscope, and the Pt particle size of Pt/GMPC was estimated through XRD analysis using a Bruker AXS D8 Advance diffractometer.

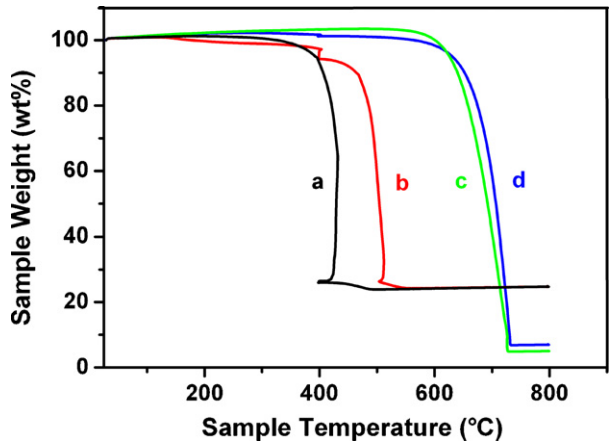

Fig. 4. TGA profiles of (a) 20 wt% Pt/XC-72, (b) 18 wt% Pt/GMPC, (c) Vulcan XC-72, and (d) GMPC.

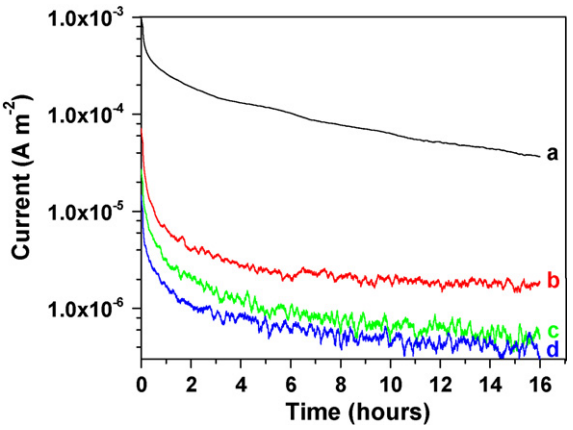

Fig. 5. Chronoamperometric curves for (a) 20 wt% Pt/XC-72, (b) 18 wt% Pt/GMPC, (c) Vulcan XC-72, and (d) GMPC, measured at 0.9 V (vs. double junction Ag/AgCl/KCl) and 25 °C in Ar-purged 0.5 M H_2SO_4.

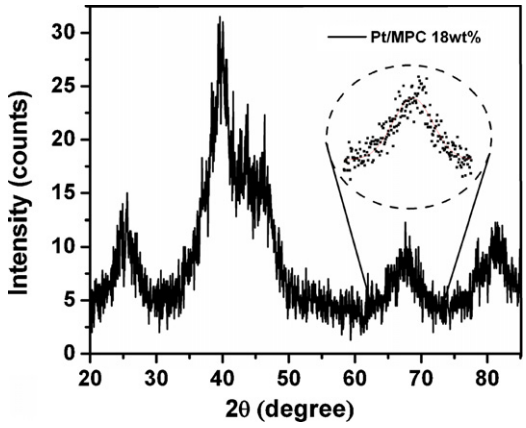

Fig. 6. XRD pattern for 18 wt% Pt/GMPC. The peak centered at a 2θ of 67.5 ° is the Pt (2 2 0) peak used to calculated particle size using Scherrer's equation.

3. Results and discussion

3.1. XRD patterns, Raman spectra, and nitrogen adsorption/desorption isotherms

It was found that the graphitic structure of the MPC was promoted after it was heat-treated (2600 °C). Before heat-treatment the MPC has two broad XRD diffraction peaks centered at 2θ of 24.4°

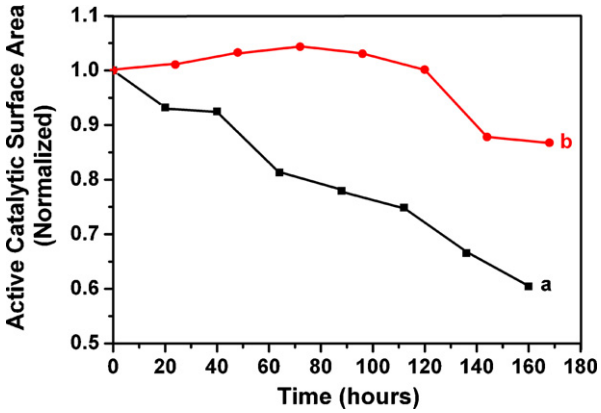

Fig. 7. Comparison of active catalytic surface area loss for (a) 20 wt% Pt/XC-72 and (b) 18 wt% Pt/GMPC at different time intervals during oxidation treatment.

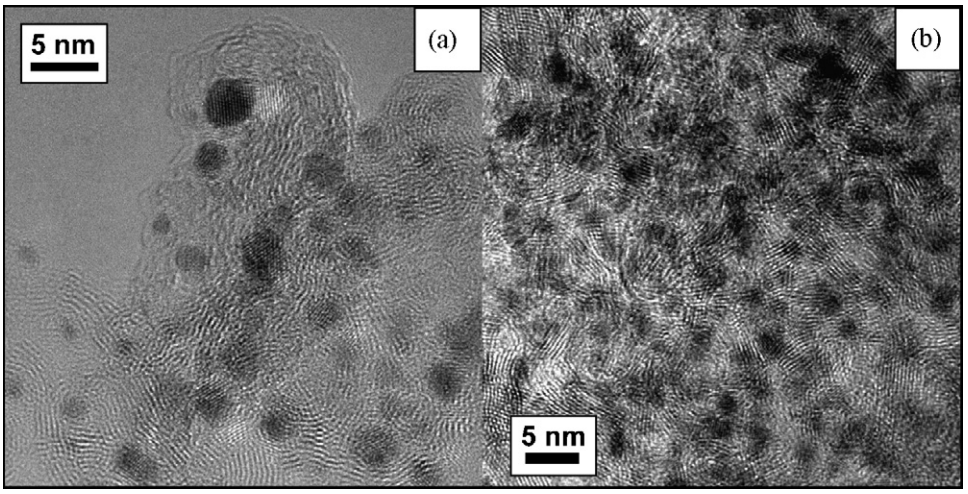

Fig. 8. High resolution TEM images of Pt/PMPC: (a) focusing on platinum particles and (b) focusing on carbon support.

and 43.6°, which are assigned to graphite (0 0 2) and (1 0 1) peaks, respectively (Fig. 1). These two peaks became sharper and narrower after the heat-treatment, indicating a more ordered graphitic structure in the heat-treated MPC. The peak positions were shifted to 25.8° and 42.6° after heat-treatment. Two additional peaks centered at 53.0° and 78.4° appeared in the XRD pattern of the heat-treated sample. These two peaks can be ascribed to the graphite (0 0 4) and (1 1 0) diffractions, respectively. The presence of (0 0 4) and (1 1 0) peaks are indicative of high crystallinity of the carbon structure [15].

Raman spectra show that sharper and narrower G and D bands appear at 1596 and 1330 cm^{-1}, respectively, after heat-treatment (Fig. 2). The relative intensity of the G band and D band (I_G/I_D) is an indication for the type of graphitic materials and a reflection of the graphitization degree [16]. The higher I_G/I_D for heat-treated MPC indicates a more ordered structure relating with graphite, as is consistent with the XRD results. The broad and short peak centered at 2790 cm^{-1} of the carbonized MPC was replaced by four peaks at 2477, 2667, 2930, and 3244 cm^{-1} in the spectrum of the heat-treated MPC. The appearance of the intense 2D band at 2667 cm^{-1} is also indicative of a higher extent of graphitic ordering [17].

The nitrogen adsorption/desorption isotherms of the MPCs before and after heat-treatment at 2600 °C are shown in Fig. 3. The BET specific surface area of the heat-treated MPC significantly dropped from 420 $m^2\ g^{-1}$, of the untreated sample, to 190 $m^2\ g^{-1}$. The mean pore diameter was slightly reduced from 9 to 8.5 nm after heat-treatment. The decrease of surface area is attributed to the elimination of micropores caused by the crystallization of the amorphous carbon.

3.2. Thermogravimetric analysis

As can be seen in Fig. 4, the Pt/GMPC experienced a 50% reduction in mass at approximately 500 °C, whereas the midpoint of the Pt/XC-72 occurred at approximately 430 °C, indicating higher oxidation stability for the Pt/GMPC. The metal loading was determined by measuring the Pt/GMPC residue (~25%) and correcting by the GMPC blank residue (~7%). The metal loading was determined to be approximately 18%.

3.3. Electrochemical properties

Fig. 5 shows the chronoamperometric curves for the various samples (i.e., Vulcan XC-72, 20 wt% Pt/XC-72, GMPC, or 18 wt% Pt/GMPC). Both Vulcan XC-72 and GMPC experience an increase in corrosion with addition of Pt. Comparing curves 5a and 5c, it can be seen that the Pt/XC-72 corrosion current increases by more than 2 orders of magnitude, but curves 5b and 5d show that the Pt/GMPC corrosion current only increases by a single order of magnitude. Curves 5a and b also indicate that the Pt/GMPC has corrosion current that is about 96% less than that of the Pt/XC-72. It is assumed that the graphitic nature of the GMPC enhances its stability. The active Pt surface area for Pt/GMPC and Pt/XC-72 was determined by cyclic voltammetry to be ~86.6 and 58.3 $m^2\ gPt^{-1}$, respectively. The particle size for each was estimated from the X-ray diffraction data using Scherrer's equation; both were found to be ~2.2 nm (Fig. 6). Based on this particle size, the theoretical maximum surface area for Pt on GMPC was calculated at 127 $m^2\ gPt^{-1}$. Comparing the theoretical maximum surface area with the measured surface area, the Pt utilization for Pt/GMPC and Pt/XC-72 was calculated at ~68 and ~46%, respectively. The Pt/XC-72 showed a 39% loss in catalytic surface area (Fig. 7a), while the Pt/GMPC exhibited an initial gain and finally a 14% loss in catalytic surface area (Fig. 7b), indicating that GMPC could potentially provide much higher durability than Vulcan XC-72.

3.4. High resolution TEM imaging

Fig. 8 shows HRTEM images of the Pt/GMPC. Fig. 8a focuses on the Pt particles, sixfold symmetry can be clearly seen in the image, indicating a high crystallinity of the Pt particles. The average particle size is approximately 2–3 nm, which is in agreement with the XRD results. Fig. 8b focuses on the carbon particles. The fringes in the HRTEM image (Fig. 8b) focusing on the carbon supports reveal layered structure with the d spacing of about 0.34 nm, indicating that the heat-treatment results in a graphitic carbon materials. Another structural feature that can be seen from the HRTEM image is that there is a considerable structural distortion, in the form of vermicular mesostructures.

4. Conclusions

GMPC with a surface area as high as 190 $m^2\ g^{-1}$ was, for the first time, successfully synthesized through high-temperature graphitization. This new porous carbon with high degree of graphitization has been demonstrated as a promising substitute for carbon black as electrocatalyst support. It has better corrosion resistance and yet it is relatively inexpensive to produce. The electrochemical oxida-

tion results reveal that GMPCs suffer minimally from the effects of ripening and catalyst loss. Future efforts should include manufacturing an MEA (metal electrode assembly) for possible single cell testing.

Acknowledgements

The work at UC was supported by Department of Energy. The work at ORNL was supported by DOE EERE. A portion of the work was conducted at the Center for Nanophase Materials Sciences, which is sponsored at ORNL by the Division of Scientific User Facilities, U.S. Department of Energy. S.D. would like to thank Dr. Nancy Dudney for the resistivity measurement of the mesoporous carbons.

References

[1] Y.Y. Shao, G.P. Yin, Y.Z. Gao, J. Power Sources 171 (2007) 558–566.
[2] P.J. Ferreira, G.J. la O', Y. Shao-Horn, D. Morgan, R. Makharia, S. Kocha, H.A. Gasteiger, J. Electrochem. Soc. 152 (2005) A2256–A2271.
[3] J. Xie, D.L. Wood, D.M. Wayne, T.A. Zawodzinski, P. Atanassov, R.L. Borup, J. Electrochem. Soc. 152 (2005) A104–A113.
[4] M. Mathias, H. Gasteiger, R. Makharia, S. Kocha, T. Fuller, J. Pisco, Abstr. Pap. Am. Chem. S 228 (2004) U653.
[5] K.H. Kangasniemi, D.A. Condit, T.D. Jarvi, J. Electrochem. Soc. 151 (2004) E125–E132.
[6] X. Wang, W.Z. Li, Z.W. Chen, M. Waje, Y.S. Yan, J. Power Sources 158 (2006) 154–159.
[7] R. Bashyam, P. Zelenay, Nature 443 (2006) 63–66.
[8] Z. Chen, W. Li, M. Waje, Y.S. Yan, Angew. Chem. Int. Ed. 46 (2007) 4060–4063.
[9] J. Zhang, K. Sasaki, E. Sutter, R.R. Adzic, Science 315 (2007) 220–222.
[10] S.H. Joo, S.J. Choi, I. Oh, J. Kwak, Z. Liu, O. Terasaki, R. Ryoo, Nature 412 (2001) 169–172.
[11] C.D. Liang, Z.J. Li, S. Dai, Angew. Chem. Int. Ed. 47 (2008) 3696–3717.
[12] Y. Meng, D. Gu, F.Q. Zhang, Y.F. Shi, H.F. Yang, Z. Li, C.Z. Yu, B. Tu, D.Y. Zhao, Angew. Chem. Int. Ed. 44 (2005) 7053–7059.
[13] C.D. Liang, K.L. Hong, G.A. Guiochon, J.W. Mays, S. Dai, Angew. Chem. Int. Ed. 43 (2004) 5785–5789.
[14] C.D. Liang, S. Dai, J. Am. Chem. Soc. 128 (2006) 5316–5317.
[15] T.W. Kim, I.S. Park, R. Ryoo, Angew. Chem. Int. Ed. 42 (2003) 4375–4379.
[16] F.B. Su, J.H. Zeng, X.Y. Bao, Y.S. Yu, J.Y. Lee, X.S. Zhao, Chem. Mater. 17 (2005) 3960–3967.
[17] S. Reich, C. Thomsen, Phil. Trans. R. Soc. Lond. A 362 (2004) 2271–2288.